

ORIGINAL ARTICLE

Intermuscular and perimuscular fat expansion in obesity correlates with skeletal muscle T cell and macrophage infiltration and insulin resistance

IM Khan^{1,2}, X-YD Perrard², G Brunner², H Lui², LM Sparks³, SR Smith³, X Wang⁴, Z-Z Shi⁴, DE Lewis⁵, H Wu^{2,6} and CM Ballantyne^{2,6,7}

BACKGROUND/OBJECTIVES: Limited numbers of studies demonstrated obesity-induced macrophage infiltration in skeletal muscle (SM), but dynamics of immune cell accumulation and contribution of T cells to SM insulin resistance are understudied.

SUBJECTS/METHODS: T cells and macrophage markers were examined in SM of obese humans by reverse transcription-PCR (RT-PCR). Mice were fed high-fat diet (HFD) for 2–24 weeks, and time course of macrophage and T-cell accumulation was assessed by flow cytometry and quantitative RT-PCR. Extramyocellular adipose tissue (EMAT) was quantified by high-resolution micro-computed tomography (CT), and correlation to T-cell number in SM was examined. CD11a^{-/-} mice and C57BL/6 mice were treated with CD11a-neutralizing antibody to determine the role of CD11a in T-cell accumulation in SM. To investigate the involvement of Janus kinase/signal transducer and activator of transcription (JAK/STAT), the major pathway for T helper 1 (T_H1) cytokine interferon- γ , in SM and adipose tissue inflammation and insulin resistance, mice were treated with a JAK1/JAK2 inhibitor, baricitinib.

RESULTS: Macrophage and T-cell markers were upregulated in SM of obese compared with lean humans. SM of obese mice had higher expression of inflammatory cytokines, with macrophages increasing by 2 weeks on HFD and T cells increasing by 8 weeks. The immune cells were localized in EMAT. Micro-CT revealed that EMAT expansion in obese mice correlated with T-cell infiltration and insulin resistance. Deficiency or neutralization of CD11a reduced T-cell accumulation in SM of obese mice. T cells polarized into a proinflammatory T_H1 phenotype, with increased STAT1 phosphorylation in SM of obese mice. *In vivo* inhibition of JAK/STAT pathway with baricitinib reduced T-cell numbers and activation markers in SM and adipose tissue and improved insulin resistance in obese mice.

CONCLUSIONS: Obesity-induced expansion of EMAT in SM was associated with accumulation and proinflammatory polarization of T cells, which may regulate SM metabolic functions through paracrine mechanisms. Obesity-associated SM 'adiposopathy' may thus have an important role in the development of insulin resistance and inflammation.

International Journal of Obesity (2015) 39, 1607–1618; doi:10.1038/ijo.2015.104

INTRODUCTION

Obesity is associated with low-grade chronic inflammation, evidenced by immune cell infiltration and activation and proinflammatory cytokine secretion in insulin-responsive tissues, which is postulated to contribute to obesity-related insulin resistance and development of type 2 diabetes.¹ Consistent with this, individuals with insulin resistance and diabetes have elevated levels of proinflammatory cytokines, such as tumor necrosis factor- α (TNF α).² Previous studies showed that obesity promotes accumulation of M1-like (CD11b+F4/80+CD11c+) macrophages in visceral adipose tissue (VAT),^{3,4} which contributes to inflammation and insulin resistance.^{5,6} Macrophage activation is largely driven by interactions with T cells, which increase in adipose tissue (AT) of obese mice.^{7–9} CD8+ T cells and proinflammatory interferon- γ (IFN γ)-producing CD4+ T cells (T helper 1 (T_H1) cells), increase in VAT of obese mice compared with lean controls,^{10–13} whereas regulatory T cells (T_{reg}) and interleukin-4-secreting CD4+ T cells (T_H2), which have anti-inflammatory effects, are reduced.^{14,15}

Increased VAT inflammatory cells impair preadipocyte/adipocyte functions, with reduced lipogenesis and increased lipolysis,^{16–18} which leads to increased circulating free fatty acids¹⁹ and subsequent ectopic fat deposition in skeletal muscle (SM).^{19,20} SM is the primary organ for maintaining whole-body glucose homeostasis, accounting for ~80% of whole-body glucose disposal.^{21,22} Lipid accumulation in SM is associated with insulin resistance in humans and animals.^{23–25} Previous studies were focused on intramyocellular lipid content (triglycerides accumulated within muscle cells) and showed associations with metabolic risk factors in humans.^{26–28} Research has also shown the existence of extramyocellular AT (EMAT) compartments. However, studies on EMAT are limited. EMAT includes intermuscular AT (IMAT), located between muscle fibers, and perimuscular AT (PMAT, or subfascial AT), primarily located around large muscles. EMAT content was increased in obese humans²⁹ and associated with systemic insulin resistance,^{30,31} but the mechanisms remain largely unknown.

¹Interdepartmental Program in Translational Biology and Molecular Medicine, Baylor College of Medicine, Houston, TX, USA; ²Division of Atherosclerosis and Vascular Medicine, Section of Cardiovascular Research, Department of Medicine, Baylor College of Medicine, Houston, TX, USA; ³Translational Research Institute for Metabolism and Diabetes, Florida Hospital, Orlando, FL, USA; ⁴Department of Translational Imaging, Houston Methodist Research Institute, Houston, TX, USA; ⁵Division of Infectious Diseases, Department of Internal Medicine, UT Health, Houston, TX, USA; ⁶Section of Leukocyte Biology, Children's Nutrition Research Center, Department of Pediatrics, Baylor College of Medicine, Houston, TX, USA and ⁷Center for Cardiovascular Disease Prevention, Methodist DeBakey Heart and Vascular Center, Houston, TX, USA. Correspondence: Dr CM Ballantyne, Baylor College of Medicine, 6565 Fannin Street, Mailstop A-601, Houston 77030, TX, USA.

E-mail: cmb@bcm.edu

Received 26 November 2014; revised 6 May 2015; accepted 17 May 2015; accepted article preview online 4 June 2015; advance online publication, 21 July 2015

Obesity causes macrophage accumulation in SM, which may contribute to SM inflammation,^{32–36} but reports are not consistent. Two groups found low levels of macrophages in SM of obese humans.^{37,38} We recently demonstrated T-cell infiltration into SM of high-fat diet (HFD)-fed mice;³⁹ however, T-cell subsets in SM of lean and obese mice and their contribution to SM inflammation and insulin resistance have not been characterized. Furthermore, the mechanism has not been elucidated. CD11a, which is also known as lymphocyte function-associated antigen-1, has an important role in lymphocyte transendothelial migration and activation.⁴⁰ CD11a was implicated in obesity-associated AT inflammation and T-cell accumulation.¹³ We thus hypothesized that CD11a mediates T-cell recruitment into SM of obese mice and that proinflammatory T_H1 cells may induce SM metabolic dysfunction. SM fibers express IFN γ receptor,⁴¹ which could further activate signal transducer and activator of transcription-1 (STAT1) via Janus kinase (JAK)-1 and -2.⁴² We thus hypothesized that T_H1 cells contribute to SM inflammation and insulin resistance via their main cytokine—IFN γ —and the JAK/STAT pathway.

In this study, we demonstrated the localization of immune cells within SM with a focus on IMAT and PMAT. We further characterized macrophages and T cells in SM of lean and obese mice and validated our results in humans. In addition, we investigated a potential mechanism of activated T cell-mediated SM inflammation and insulin resistance.

MATERIALS AND METHODS

Mice

Male C57BL/6J wild-type (WT) mice were obtained from The Jackson Laboratory (Bar Harbor, ME, USA). Mice were fed normal chow diet (ND; 12% kcal from fat; Picolab Rodent Diet 5010, Purina Mills) after weaning until 8 weeks old. Starting at 8 weeks of age, mice were fed western HFD (41% kcal from fat; Dyets 112734, Dyets Inc., Bethlehem, PA, USA) for 2–24 weeks or maintained on ND for the same period. CD11a-deficient (CD11a^{-/-})¹³ and C57BL/6NHsd control mice (Harlan Laboratories, Indianapolis, IN, USA) were fed ND or HFD for 16 weeks. Animal studies and procedures were approved by the Institutional Animal Care and Use Committee of Baylor College of Medicine. For micro-computed tomography (micro-CT) studies, C57BL/6J mice fed ND or a diet with 60% kcal from fat (60% HFD; D12492, Research Diets) for 12 weeks were donated by Willa Hsueh (Houston Methodist Research Institute, Houston, TX, USA). No randomization was used to allocate the animals to experimental groups. The investigator was not blinded to the group allocation.

Micro-CT studies

Mice were scanned with high-resolution micro-CT (Siemens Inveon Preclinical Multimodel SPECT/CT) using the Inveon Acquisition Workplace software package (Siemens, Erlangen, Germany). A filtered back projection algorithm was used for reconstruction, resulting in reconstructed isotropic voxel size of 0.205 mm. Excised mouse legs were imaged at higher resolution (isotropic voxel size = 0.108 mm).

Micro-CT data for mice were analyzed with custom-built software implemented in Matlab Version 7.8.0 (64-bit). AT was quantified semiautomatically using region of interest-based approach.⁴³ IMAT and PMAT were quantified in three micro-CT slices of the thigh (Supplementary Figures 4 and 5) and summed in mm². Calf IMAT/PMAT was obtained from a single slice at midcalf. Abdominal visceral AT (VAT) and abdominal subcutaneous adipose tissue (SAT) were quantified in one abdominal micro-CT slice in the region between L4 and L5 (Supplementary Figure 6).

Metabolic studies

Plasma glucose and insulin from mice after 6-h fast were measured at Baylor College of Medicine Mouse Metabolism Core. Insulin resistance was estimated by homeostasis model assessment of insulin resistance.³⁹ Fasted mice were injected intraperitoneally with 1.5 U kg⁻¹ regular human insulin or saline. After 10 min, mice were euthanized, and quadriceps muscle tissues harvested.

Flow cytometry

The whole quadriceps SM (referred to as 'SM'), which included muscle fibers, IMAT and PMAT, from mouse hind legs was minced and digested at 37 °C with 450 U ml⁻¹ collagenase type I (Worthington Biochemical Corporation, Lakewood, NJ, USA) for 45 min. Digested tissues were strained through 100 μ m-pore filters, and cells recovered by centrifugation. Cells were incubated in CD16/CD32 antibody (BD Pharmingen, San Diego, CA, USA, catalog #553142) to block Fc receptors and stained with Fixable Viability Dye eFluor 780 (eBioscience, San Diego, CA, USA, catalog #65-0865) and antibodies specific for CD45 (BD Pharmingen, catalog #553080), CD3 (BD Pharmingen, catalog #553066), CD4 (BD Pharmingen, catalog #553052), CD8 (BD Pharmingen, catalog #561094), CD11b (BD Pharmingen, catalog #553311), F4/80 (eBioscience, catalog #17-4801), CD11c (eBioscience, catalog #45-0114) and CD25 (eBioscience, catalog #17-0251), or isotype controls. For intracellular staining, cells were incubated with Leukocyte Activation Cocktail with BD GolgiPlug (BD Pharmingen) in complete Roswell Park Memorial Institute medium (Invitrogen, Carlsbad, CA, USA) containing 10% fetal bovine serum for 5 h at 37 °C. Cell suspensions were fixed and permeabilized with BD Cytofix/Cytoperm kit (BD Biosciences, San Diego, CA, USA) and stained with anti-IFN γ (BD Pharmingen, catalog #554412). To detect T_{reg} cells, muscle cells were incubated in fixation/permeabilization solution (eBioscience) for 1 h at room temperature, washed and stained with anti-FoxP3 (eBioscience, catalog #12-5773). Flow cytometry analysis was performed with Beckman Coulter Kaluza 1.2 software.

Immunohistochemistry

Quadriceps tissues were fixed in Z-fix (Anatech Ltd, Battle Creek, MI, USA), embedded in paraffin and sectioned for staining with hematoxylin/eosin, 1:50 dilution of monoclonal antibody to Mac3 (clone M3/84, BD Pharmingen, catalog #550292), or immunoglobulin G-isotype control (BD Pharmingen, catalog #559072) followed by biotinylated anti-rat immunoglobulin G antibody (Vector Laboratories, Burlingame, CA, USA, catalog #BA-4001), or 1:20 dilution of polyclonal antibody to CD3 (Abcam, Cambridge, UK, catalog #ab5690), followed by biotinylated goat anti-rabbit antibody (Abcam, catalog #ab128978). Tissues were incubated with Vectorstain Elite ABC kit and DAB substrate (Vector Laboratories).

In vivo neutralization of CD11a

C57BL/6NHsd mice on HFD for 12 weeks were injected intraperitoneally with 200 μ g KBA (neutralizing antibody to mouse CD11a, rat IgG2a) or rat IgG2a isotype control (eBioscience, catalog #16-4321) on alternate days for nine injections. Mice were killed 2 days after last injection, and quadriceps tissues harvested for reverse transcription-PCR (RT-PCR) and flow cytometry.

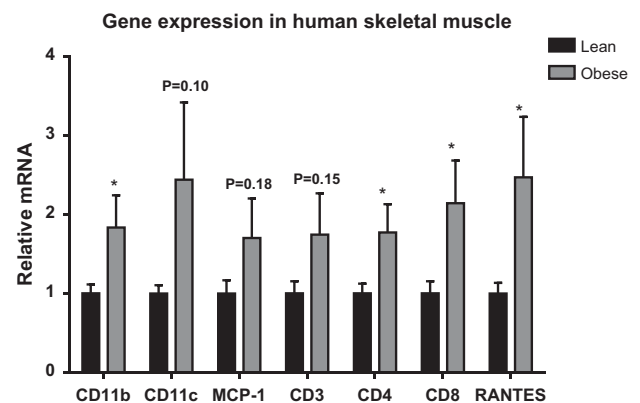


Figure 1. Macrophages and T cells were elevated in SM of obese humans. Quantitative RT-PCR was performed to analyze the expression of macrophage markers (CD11b, CD11c and MCP-1) and T-cell markers (CD3, CD4, CD8 and RANTES) in vastus lateralis muscle biopsies of lean ($n=15$) and obese ($n=12$) individuals. * $P < 0.05$ compared with lean controls.

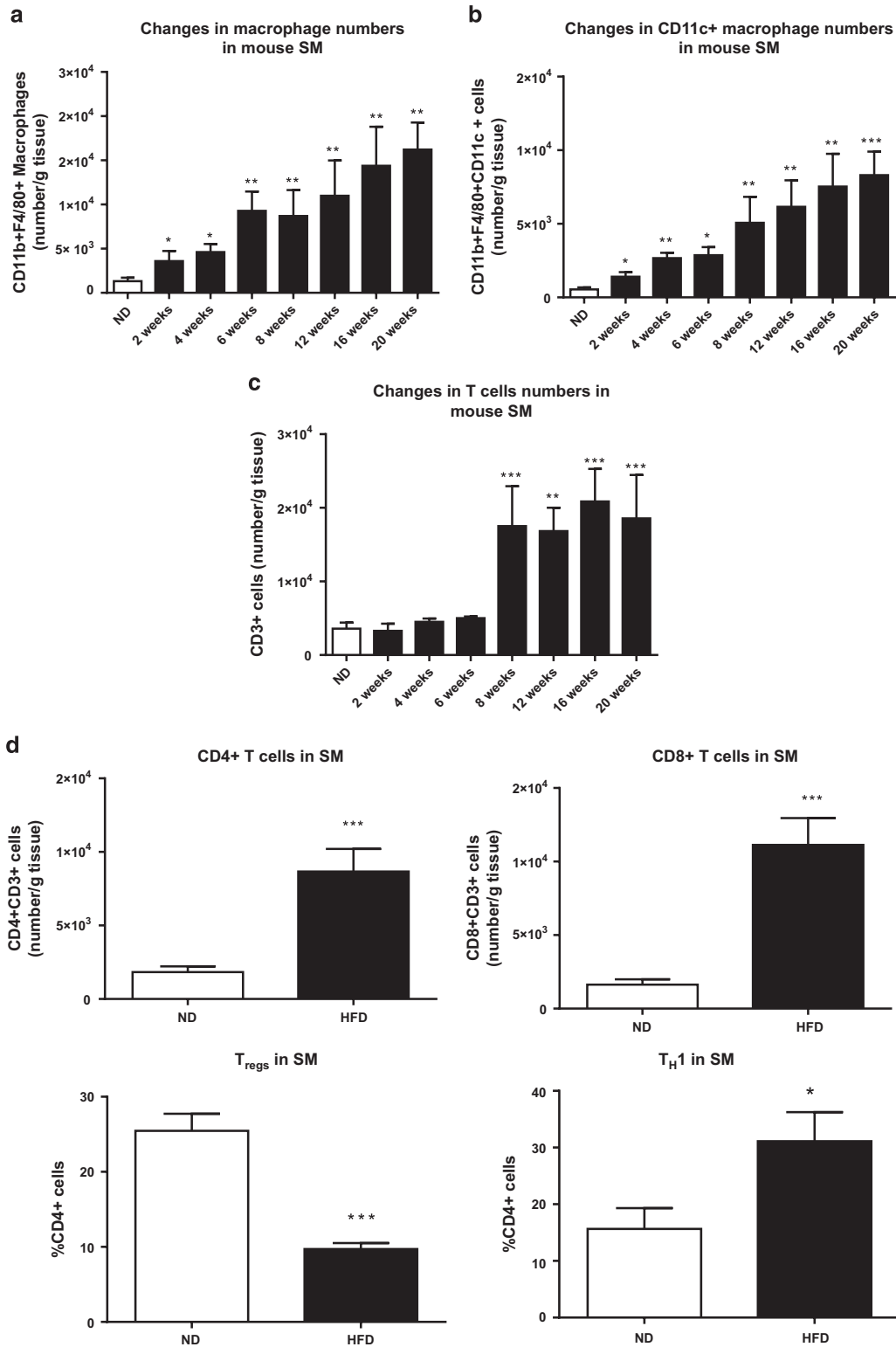


Figure 2. Macrophages and T cells increased during the course of HFD feeding. SM, consisting of muscle fibers, IMAT and PMAT, was harvested from hind legs, enzymatically digested and analyzed by flow cytometry to quantify numbers of (a) CD11b+F4/80+ macrophages, (b) CD11b+F4/80+CD11c+ proinflammatory macrophages and (c) CD3+ T cells per gram tissue. (d) Quantification of T-cell subsets in SM of lean and obese mice, including CD4+ T-cell number and CD8+ T-cell number per gram tissue ($n = 10$ mice per group), and CD4+CD25+FoxP3+ (T_{reg}) cells ($n = 5$ mice per group) and CD4+IFN γ + (T_H1) cells ($n = 6$ mice per group) expressed as % CD4+ T cells. * $P < 0.05$, ** $P < 0.01$, *** $P < 0.001$ compared with ND.

Baricitinib treatment

Mice fed HFD for 2 months were orally administered vehicle or 10 mg kg⁻¹ body weight INCB028050 (baricitinib; MedChemexpress, Monmouth Junction, NJ, USA) suspended in 0.5% methylcellulose once daily for 3 weeks. On day 18 after the initiation of treatment, mice were fasted for 6 h followed by intraperitoneal injection of 1.5 U kg⁻¹ regular human insulin for insulin tolerance test. On day 22, mice were killed, and SM and perigonadal AT collected for RT-PCR and flow cytometry.

Naive CD4⁺ T cell and T_H1 cell culture

Naive CD4⁺ T cell- and T_H1-conditioned media were obtained as described.³⁹

Cell culture

Confluent C2C12 cells (ATCC) were induced to differentiate by replacing Dulbecco's Modified Eagle Medium supplemented with 10% fetal bovine serum (HyClone, Fisher Scientific, Pittsburgh, PA, USA) with 2% horse serum Dulbecco's Modified Eagle Medium. After 4 days, differentiated myotubes were treated for 48 h with naive CD4⁺ T cell- or T_H1-conditioned medium with or without 10 ng ml⁻¹ anti-IFN γ antibody or 1 μ M JAK inhibitor I (Calbiochem, EMD Millipore Corporation, Billerica, MA, USA), and messenger RNA (mRNA) was isolated. In a separate experiment, after treatment for 48 h in serum-free medium, C2C12 myotubes were treated with PBS or 100 nm insulin for 15 min, lysed and collected for western blotting.

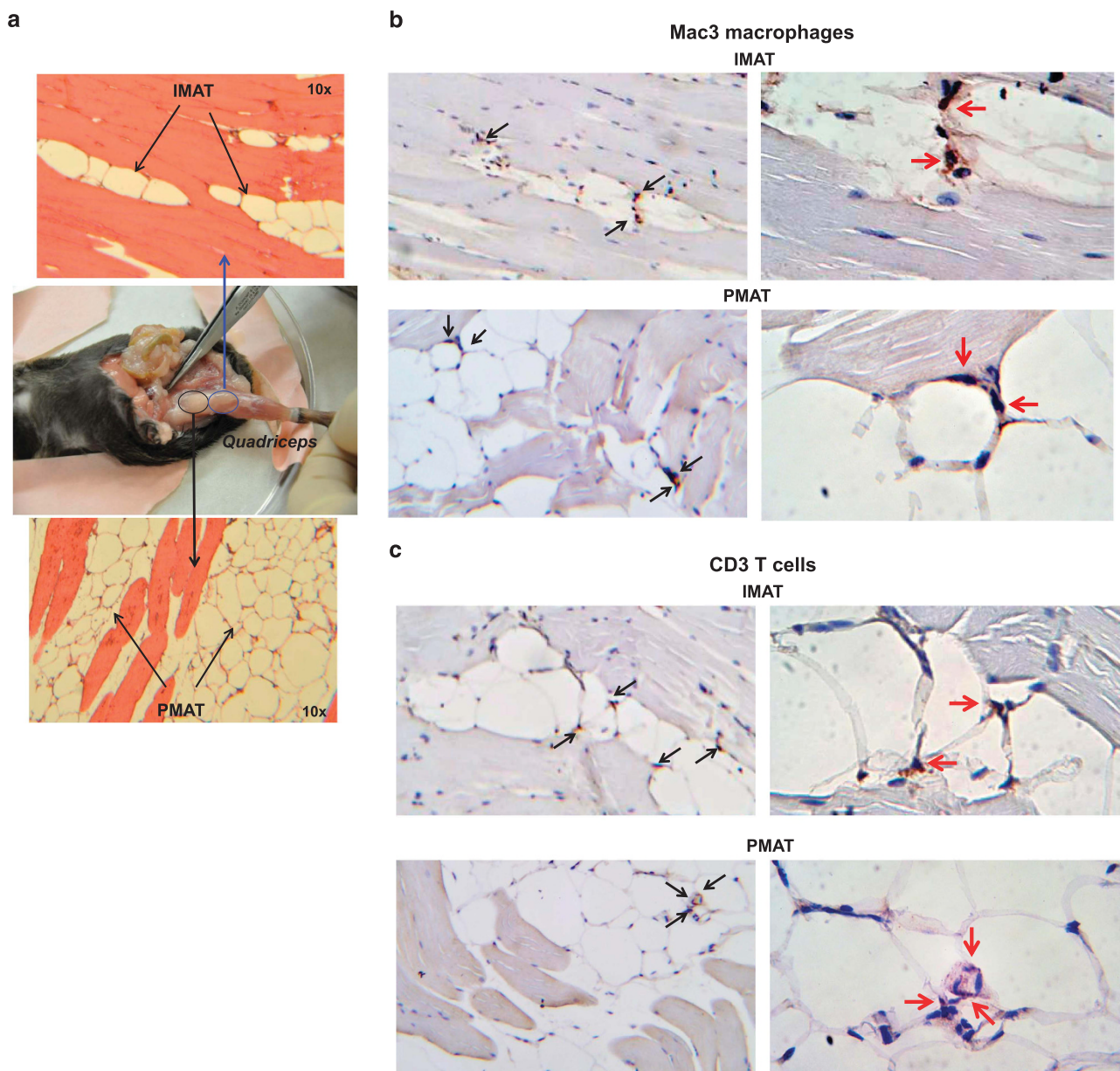


Figure 3. Macrophages and T cells accumulated in PMAT and IMAT of HFD-fed mice. Quadriceps SM with IMAT and adherent PMAT were harvested from ND- and HFD-fed mice. (a) Location and representative H&E staining of quadriceps with PMAT and IMAT from HFD-fed mice, $\times 10$ magnification. Immunohistochemical staining of SM for (b) macrophages (Mac3, arrows) and (c) T cells (CD3, arrows) under $\times 10$ magnification (left panel) and $\times 40$ magnification (right panel). RNA was isolated from PMAT and 'muscle', which includes muscle fiber and IMAT, of ND- and HFD-fed mice ($n = 10$ mice per group). (d) Quantitative RT-PCR analysis of macrophage markers (F4/80 and CD11c), T-cell markers (CD3, CD4 and CD8) and cytokines/chemokines (TNF α , IFN γ , MCP-1 and RANTES). * $P < 0.05$, ** $P < 0.01$, *** $P < 0.001$. Student's *t*-test was performed to compare gene expression in PMAT or 'muscle' between ND and HFD groups; two-way ANOVA was used to assess HFD-induced changes between PMAT and 'muscle'.

d

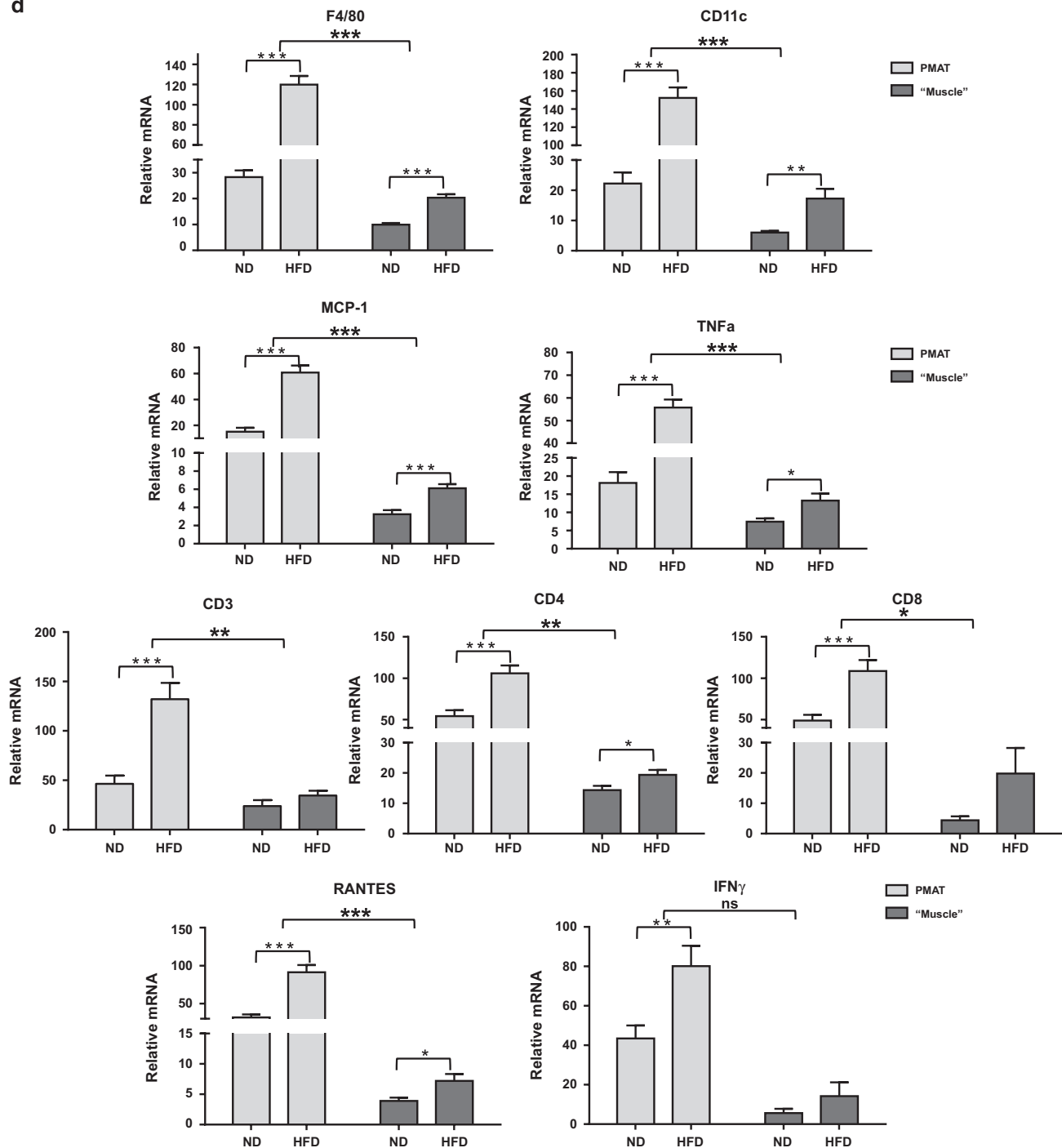


Figure 3. (Continued)

Human studies

Lean (BMI = $21.7 \pm 1.7 \text{ kg m}^{-2}$; $n = 15$) and obese (BMI = $36.0 \pm 4.8 \text{ kg m}^{-2}$; $n = 12$) normoglycemic (hemoglobin A1c $\leq 6.5\%$) participants in a cross-sectional study (ORIGINS) at the Translational Research Institute for Metabolism and Diabetes (Supplementary Table 1) had blood drawn and underwent biopsy of the vastus lateralis. The study was approved by the Florida Hospital Institutional Review Board. All subjects signed informed consents prior to the study.

RNA isolation and quantitative RT-PCR

Total RNA was isolated using TRIzol reagent (Invitrogen) per manufacturer's instructions from SM (including muscle fiber, IMAT and PMAT), 'muscle' (including muscle fiber and IMAT) and PMAT.

Gene expression was examined by quantitative RT-PCR and expressed as relative mRNA levels compared with 18S ribosomal RNA internal control. Samples with low quantity of 18S were excluded from the analysis.

Western blotting

SM and cells were homogenized in Complete Lysis-M ethylenediaminetetraacetic acid-free buffer (Roche Applied Science, Indianapolis, IN, USA). Protein concentration was measured using the BCA protein assay kit (Pierce Biotechnology, Rockford, IL, USA). Proteins were subjected to electrophoresis in polyacrylamide 4–12% Bis-Tris Gels (Invitrogen) and transferred to polyvinylidene difluoride membranes. After blocking with 5% bovine serum albumin in tris-buffered saline containing 0.1% Tween 20 for 2 h,

membranes were immunoblotted with serine⁴⁷³-phosphorylated Akt (P-Akt), tyrosine⁷⁰¹-phosphorylated STAT1 (P-STAT1), total Akt or total STAT1 antibodies (Cell Signaling Technology, Danvers, MA, USA). After incubation with secondary antibody conjugated to horseradish peroxidase, antibody-bound proteins were detected using Pierce ECL 2 Substrate reagent (Thermo Fisher Scientific, Waltham, MA, USA). Bands were scanned and quantified using a STORM 840 (Amersham Biosciences, Piscataway, NJ, USA).

Statistics

All data are represented as means \pm s.e.m. Statistical analyses were performed using GraphPad Prism 5.0 and SAS 9.3. All data were tested for normal distribution and equivalence of variances. Comparisons between two groups were made using Student's *t*-test for samples with normal distribution and equivalence of variances. Otherwise, nonparametric Mann-Whitney tests were used. Significance was defined as

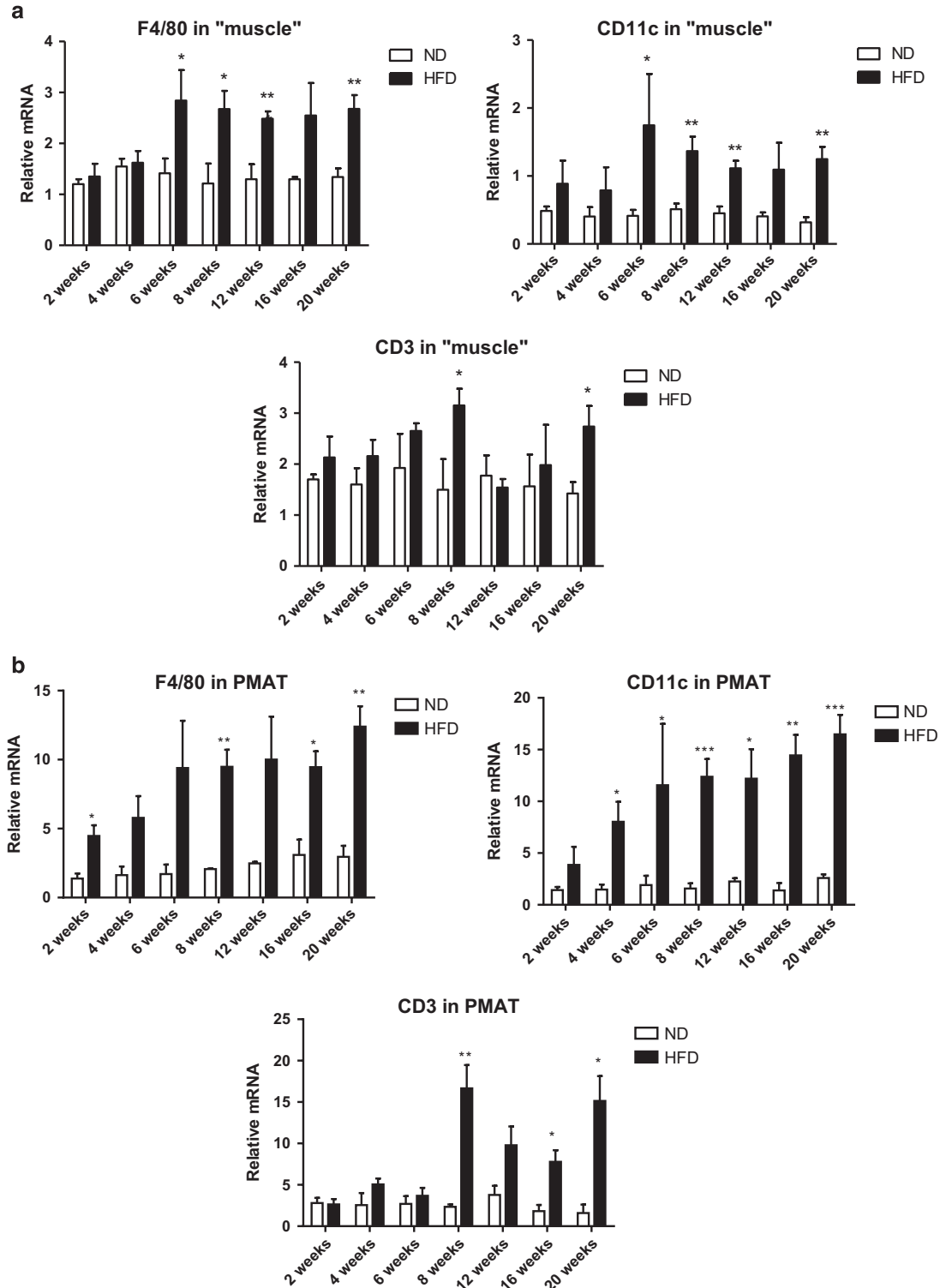


Figure 4. EMAT expansion during 20 weeks of HFD is accompanied by inflammatory cell infiltration. Expression of genes encoding macrophage markers F4/80 and CD11c and T-cell marker CD3 in (a) quadriceps 'muscle' and (b) 'PMAT' from mice fed ND or HFD for 2–20 weeks ($n = 3–6$ mice per group). * $P < 0.05$, ** $P < 0.01$, *** $P < 0.001$ for comparisons between diets at the indicated time point.

$P \leq 0.05$. Data for IMAT/PMAT, VAT and SAT are not normally distributed and are reported as median (interquartile range). P -values were computed using the nonparametric Kruskal-Wallis test. For correlation analysis, Pearson correlation coefficients were calculated. Two-way analysis of variance was used to assess the HFD-induced changes in gene expression between PMAT and 'muscle' and the response to insulin in vehicle control- and baricitinib-treated mice.

RESULTS

T-cell and macrophage markers are upregulated in SM of obese humans

We first examined obesity-induced changes in inflammatory markers in human SM by comparing the expression of T-cell and macrophage markers in vastus lateralis biopsies from lean and obese normoglycemic humans (Supplementary Table 1) by RT-PCR. Consistent with previous studies,^{35,44} macrophage marker CD11b was significantly increased in SM of obese humans compared with lean controls (Figure 1). Proinflammatory CD11c and MCP-1 gene expression was also higher, although those results were not statistically significant because of large variation in the obese group. In addition, we observed the upregulation of T-cell markers. CD4, CD8 and RANTES were all significantly increased in SM of obese humans (Figure 1). Our results thus suggest that obesity in humans results in increases in both macrophage and T-cell markers.

Macrophage infiltration precedes T-cell accumulation in SM during the development of obesity in mice

Next, using HFD-induced obese mouse models, we further examined dynamic changes of immune cells in SM. Similarly to that in obese humans, HFD feeding for 12 weeks in mice resulted in the upregulation of macrophage (F4/80, CD11c) and T-cell (CD3, CD8) markers in quadriceps SM (Supplementary Figure 1), consistent with other reports.^{32,35,36,39} SM isolated from these HFD-fed mice also had significant increases in the expression of inflammatory cytokines (IL-12 β , IL-18, TNF α and IFN γ) and chemokines (MCP-1 and RANTES) (Supplementary Figure 1). We then examined dynamic changes of immune cells in SM as obesity progressed by comparing mice fed HFD for 2–20 weeks with age-matched ND-fed mice. We performed flow cytometric analysis by gating the viable CD45+ cells and further identified CD11b+F4/80+ cells (total macrophages) and CD11c+ cells (M1-like macrophages) within the CD11b+F4/80+ fraction (Supplementary Figure 2A). In the viable CD45+ cells, we quantified CD3+ T cells and CD4+ and CD8+ subsets within the CD3+ fraction (Supplementary Figure 2B). Total macrophage and M1 macrophage numbers were significantly upregulated within 2 weeks on HFD (Figures 2a and b). In contrast, T-cell numbers were unchanged during the first 6 weeks, but markedly increased at 8 weeks after HFD initiation (Figure 2c). We then characterized subsets of SM-associated T cells in mice fed HFD or ND for 12 weeks. Both CD4+ and CD8+ T-cell numbers were significantly upregulated in SM of obese mice (Figure 2d). We further made the

novel observation that the proportion of CD25+FoxP3+ T_{reg} was diminished 2.5-fold within the CD4+ T-cell population. We also confirmed our previous results showing the induction of proinflammatory T_H1 cells in SM of HFD-fed compared with ND-fed mice³⁹ (Figure 2d).

T cells and macrophages are predominantly located in PMAT and IMAT

In addition to muscle fibers, quadriceps SM consists of AT between muscle fibers (IMAT) and directly connected to muscle (PMAT) (Figure 3a). Immunohistochemistry on quadriceps sections from ND-fed mice showed that Mac3+ macrophages and CD3+ T cells are few and located between muscle fibers (Supplementary Figure 3). In contrast, SM of mice that were fed HFD for 12 weeks had increased Mac3+ macrophage and CD3+ T-cell numbers, which were primarily localized in PMAT and IMAT in clusters surrounding adipocytes (crown-like structures) (Figures 3b and c). Next, we separated the quadriceps SM into PMAT and 'muscle' and compared the inflammatory gene expression. Although PMAT contained only the AT, 'muscle' was a combination of muscle fibers and IMAT, because of difficulty in separating IMAT from muscle fibers. RT-PCR revealed upregulation of macrophage-associated F4/80, CD11c, MCP-1 and TNF α and T cell-associated CD3, CD4, CD8, RANTES and IFN γ in both 'muscle' and PMAT of obese mice compared with 'muscle' and PMAT of lean mice (Figure 3d). Furthermore, in both obese and lean mice, most of the inflammatory markers were higher in PMAT than in 'muscle', which also included IMAT. However, it was difficult to examine whether these inflammatory marker levels were different between PMAT and IMAT, as it was not feasible to separate IMAT from muscle fibers and IMAT accounted for only a small portion of 'muscle'. In addition, the HFD-induced increases in the inflammatory markers were greater in PMAT than in 'muscle' (Figure 3d). Examination of dynamic changes showed that F4/80 and CD11c expression was unchanged in 'muscle' during 4 weeks on HFD and significantly increased after 6 weeks on HFD compared with ND (Figure 4a). In contrast, within PMAT, F4/80 mRNA level was significantly higher after only 2 weeks, and CD11c mRNA level was markedly upregulated at 4 weeks on HFD (Figure 4b). Initial CD3 expression was comparable between lean and obese mice for the first 6 weeks in both 'muscle' and PMAT and increased 17-fold in PMAT but only twofold in 'muscle' at 8 weeks on HFD (Figures 4a and b). Our results suggest that in obesity, SM inflammation primarily occurs in SM AT depots, with early increases in macrophages, followed by T-cell accumulation.

IMAT and PMAT accumulation is highly correlated with insulin resistance in obesity

Next, we measured the amount of IMAT/PMAT in the thigh and calf, VAT and SAT of mice by micro-CT (Supplementary Figures 4–6). IMAT/PMAT increased 25-fold, whereas VAT increased sixfold, and SAT increased ninefold in obese mice compared with lean mice (Supplementary Table 2). Thigh and calf IMAT/PMAT and total

Table 1. Pearson correlation coefficients for extramyocellular adipose tissue and insulin resistance

Adipose tissue	Body weight	Abdominal VAT	Abdominal SAT	Glucose	Insulin	HOMA-IR	P-Akt/Akt
Thigh IMAT/PMAT	0.827 ($P=0.011$)	0.799 ($P=0.018$)	0.649 ($P=0.082$)	0.888 ($P=0.003$)	0.610 ($P=0.108$)	0.729 ($P=0.040$)	-0.794 ($P=0.060$)
Calf IMAT/PMAT	0.738 ($P=0.037$)	0.697 ($P=0.055$)	0.754 ($P=0.031$)	0.456 ($P=0.256$)	0.923 ($P=0.001$)	0.863 ($P=0.006$)	-0.547 ($P=0.261$)
Total IMAT/PMAT	0.894 ($P=0.0028$)	0.859 ($P=0.006$)	0.740 ($P=0.036$)	0.884 ($P=0.004$)	0.743 ($P=0.035$)	0.834 ($P=0.010$)	-0.827 ($P=0.042$)
Abdominal VAT	0.988 ($P<0.001$)	—	0.917 ($P=0.001$)	0.693 ($P=0.057$)	0.789 ($P=0.020$)	0.784 ($P=0.021$)	-0.968 ($P=0.002$)

Abbreviations: HOMA-IR, homeostasis model assessment of insulin resistance; IMAT/PMAT, intermuscular adipose tissue/perimuscular adipose tissue; P-Akt, serine⁴⁷³-phosphorylated Akt; SAT, abdominal subcutaneous adipose tissue; VAT, abdominal visceral adipose tissue. Pearson correlation coefficients were computed with SAS 9.3 (pooled analysis, $n=8$).

IMAT/PMAT were positively correlated with body weight, abdominal VAT and SAT (Table 1). Obese mice were more insulin resistant by assessment of increased homeostasis model assessment of insulin resistance (Supplementary Figure 7A) and decreased insulin-stimulated P-Akt level in quadriceps SM compared with lean mice (Supplementary Figure 7B). Total IMAT/PMAT was significantly positively correlated with fasting glucose, fasting insulin and homeostasis model assessment of insulin resistance and was negatively associated with P-Akt level in SM (Table 1). Total IMAT/PMAT was positively correlated with T-cell number ($r=0.724$; $P=0.042$). Our data suggested that accumulation of IMAT/PMAT and expansion of SAT and VAT depots correlates with SM inflammation and insulin resistance.

T-cell recruitment into SM in obesity is mediated by CD11a

To study the mechanism of T-cell accumulation in SM in obesity, we tested the involvement of CD11a using HFD-fed CD11a^{-/-} mice. Compared with obese WT, obese CD11a^{-/-} mice had significantly reduced expression of CD3, RANTES, MCP-1 and TNF α in SM (Figure 5a). Flow cytometric analysis also revealed significant reduction in the number of T cells, including CD4⁺ and CD8⁺ T cells. On the other hand, macrophage number was not different between the two groups of mice (Figure 5b). Similarly, neutralization of CD11a with KBA in obese WT mice reduced CD8⁺ T-cell numbers in SM without affecting macrophage numbers, as measured by flow cytometry (Figure 5c). Although CD11a blockade did not change CD3 expression in 'muscle', CD3 mRNA level was markedly reduced in PMAT (Figure 5d). All these data suggest involvement of CD11a in T-cell accumulation in SM, particularly SM-associated fat depots.

T_H1 cells directly impair SM cell metabolic functions through IFN γ -induced JAK/STAT pathway

Because of increased levels of T_H1 cells and T_H1 cytokine IFN γ in SM of obese mice, we examined effects of T_H1 on SM cell metabolic functions and inflammation. IFN γ is known to signal through the JAK/STAT1 pathway involving activation of JAK1/JAK2 kinases. Consistently, P-STAT1 protein levels were increased in SM of HFD-fed WT mice compared with lean WT mice (Supplementary Figure 8A), whereas obese mice with ablation of T_H1 (TCRb^{-/-} mice)³⁹ did not show increased P-STAT1 in SM (data not shown). To further study the effect of T_H1 cells on muscle inflammation and metabolic functions, we performed *in vitro* experiments using murine C2C12 myofibers. Treatment of differentiated C2C12 cells with T_H1-conditioned medium for 48 h significantly upregulated MCP-1, RANTES, IL-6 and TNF α expression (Supplementary Figure 8B) and increased both STAT1 mRNA and P-STAT1 protein levels (Supplementary Figure 8C). The addition of anti-IFN γ antibody attenuated T_H1-induced inflammation and P-STAT1 induction (Supplementary Figures 8B–C), indicating the effect of T_H1 cells was mainly attributable to IFN γ . T_H1 treatment also caused significant reductions in insulin-stimulated P-Akt (Supplementary Figure 8D), suggesting insulin resistance, in C2C12 myocytes. Treatment of C2C12 cells with nonspecific JAK inhibitor reduced T_H1-induced P-STAT1 (Supplementary Figure 8D), attenuated T_H1-mediated upregulation of proinflammatory IL-6, TNF α , MCP-1 and RANTES (Supplementary Figure 8B) and improved T_H1-induced insulin resistance, as shown by increased P-Akt level (Supplementary Figure 8D).

JAK1/JAK2 inhibitor baricitinib reduces T-cell accumulation and activation in SM and improves insulin sensitivity

We next examined effects of T_H1 cell/cytokine-pathway on inflammation and metabolic functions *in vivo* by treating obese mice with baricitinib, a selective JAK1/JAK2 inhibitor, which blocks IFN γ -induced signaling.⁴⁵ Treatment of obese WT mice with

baricitinib for 3 weeks reduced the expression of T cell-related markers, such as CD4, CD8, RANTES, IL-2 and IFN γ , in both 'muscle' and PMAT (Figures 6a and b) and significantly decreased the number of T cells, including CD4⁺ and CD8⁺ T cells, but not macrophages, in SM (Figure 6c). These changes were accompanied by improved insulin resistance in HFD-fed mice after baricitinib treatment, compared with vehicle, indicated by significantly enhanced blood glucose clearance following an insulin injection (Figure 6d). Together these results provide the first *in vivo* evidence that T_H1 cells may induce SM inflammation and insulin resistance involving a JAK/STAT mechanism.

DISCUSSION

Our results suggested that the AT depots associated with SM—IMAT and PMAT—may have a role in obesity-induced SM inflammation and insulin resistance. We showed that T cells, together with macrophages, primarily accumulate in IMAT/PMAT. The increase in macrophage numbers in SM-associated IMAT/PMAT occurs during the early stage of obesity and precedes T-cell accumulation. The induction of T cells in SM of obese mice was reduced by inhibition of CD11a. T cells polarized into proinflammatory T_H1 in obese conditions, whereas T_{reg} cells were diminished. T_H1 cells secrete IFN γ and induce myocyte inflammation and insulin resistance via activation of the JAK/STAT pathway. Indeed, inhibition of the JAK/STAT pathway reduced inflammatory pathway activation and the production of chemokines in cultured myocytes. *In vivo*, targeting the JAK/STAT pathway using the JAK1/JAK2 inhibitor baricitinib attenuated obesity-associated RANTES, IL-2 and IFN γ expression, reduced T-cell infiltration in both 'muscle' and PMAT and improved insulin sensitivity.

We show here that in addition to macrophage accumulation previously described in the literature,^{1,20} SM in obesity was also characterized by increased T-cell accumulation. T cells were significantly increased after 8 weeks on HFD, whereas macrophages were upregulated after only 2 weeks on HFD. Our results thus suggest an early infiltration of macrophages in obese SM, followed by accumulation of T cells, which may contribute to SM metabolic dysfunction at a later stage of obesity. We previously reported that mice lacking $\alpha\beta$ T cells did not show macrophage infiltration in SM upon HFD feeding.³⁹ We speculate that T cells residing in SM of lean WT mice may have an important role in attracting early infiltration of macrophages into SM during obesity and that deficiency of 'resident' T cells in SM of $\alpha\beta$ cell-deficient mice may have contributed to the lack of macrophage infiltration into SM of these mice.

Although accumulation of immune cells was also observed between muscle bundles, macrophages and T cells were primarily located in EMAT of obese mice. This observation may explain the inconsistent results of human studies reported in the literature. Low macrophage and T-cell numbers in human SM biopsies may be attributable to the location of biopsies and whether the overlying PMAT was trimmed before analysis. These results are important for future research done in human subjects. Similar to VAT, the majority of immune cells in IMAT/PMAT were located within crown-like structures.⁴⁶ Consistent with our histological findings, we showed significantly higher proinflammatory cytokine and chemokine gene expression in PMAT compared with 'muscle'. The induction of macrophage markers in PMAT occurred earlier in the course of HFD feeding compared with 'muscle' connected to it, suggesting that infiltration of immune cells into EMAT may initiate SM inflammation in obesity.

T cells and macrophages residing in PMAT and IMAT may exert effects on the neighboring myocytes via a paracrine mechanism and induce the expression of proinflammatory chemokines, such as MCP-1 and RANTES, further mediating blood monocyte and T-lymphocyte migration into SM.^{47,48} T-cell trafficking may be mediated by a combination of chemokines and adhesion

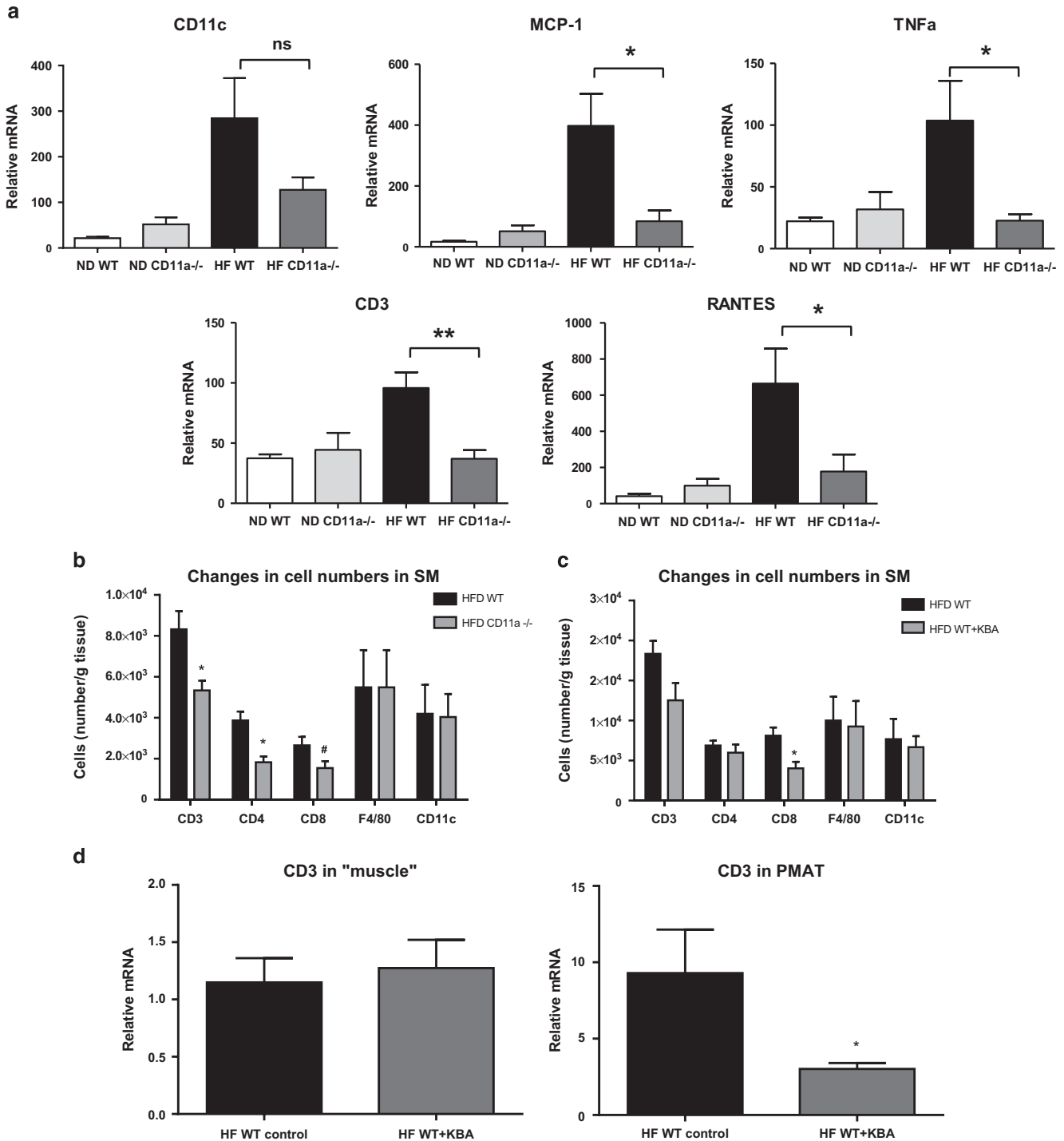


Figure 5. CD11a deficiency reduced obesity-associated SM inflammation and T-cell accumulation. **(a)** mRNA levels of inflammatory genes in SM of WT and CD11a^{-/-} mice examined by quantitative RT-PCR ($n=8$ mice per group). **(b)** Numbers of CD3⁺, CD8⁺ and CD4⁺ T cells and CD11b⁺F4/80⁺ and CD11b⁺F4/80⁺CD11c⁺ macrophages per gram SM tissue harvested from HFD-fed CD11a^{-/-} and WT mice ($n=4$ mice per group). HFD-fed WT mice were injected with KBA, a neutralizing anti-mouse CD11a antibody, or IgG control every other day for nine times ($n=4$ mice per group), and SM from hind legs was harvested to analyze **(c)** the number of CD3⁺, CD8⁺ and CD4⁺ T cells and CD11b⁺F4/80⁺ and CD11b⁺F4/80⁺CD11c⁺ macrophages per gram tissue by flow cytometry ($n=8$ mice per group) and **(d)** relative mRNA levels of CD3, a total T-cell marker, in 'muscle' (left panel) and in PMAT (right panel). # $P=0.08$, * $P<0.05$, ** $P<0.01$ compared with HFD WT (control).

molecules, such as CD11a.⁴⁹ CD11a^{-/-} mice, as well as mice treated with CD11a-neutralizing antibody, had decreased T-cell content, likely attributable to reduced T-cell migration into SM. Obese CD11a^{-/-} mice had attenuated inflammatory gene

expression, which may reflect the effect of T cells on macrophage and SM cell cytokine production, as we recently reported in VAT.^{13,39} Our findings not only provide a potential mechanism of T-cell transmigration into SM, specifically EMAT, but also show an

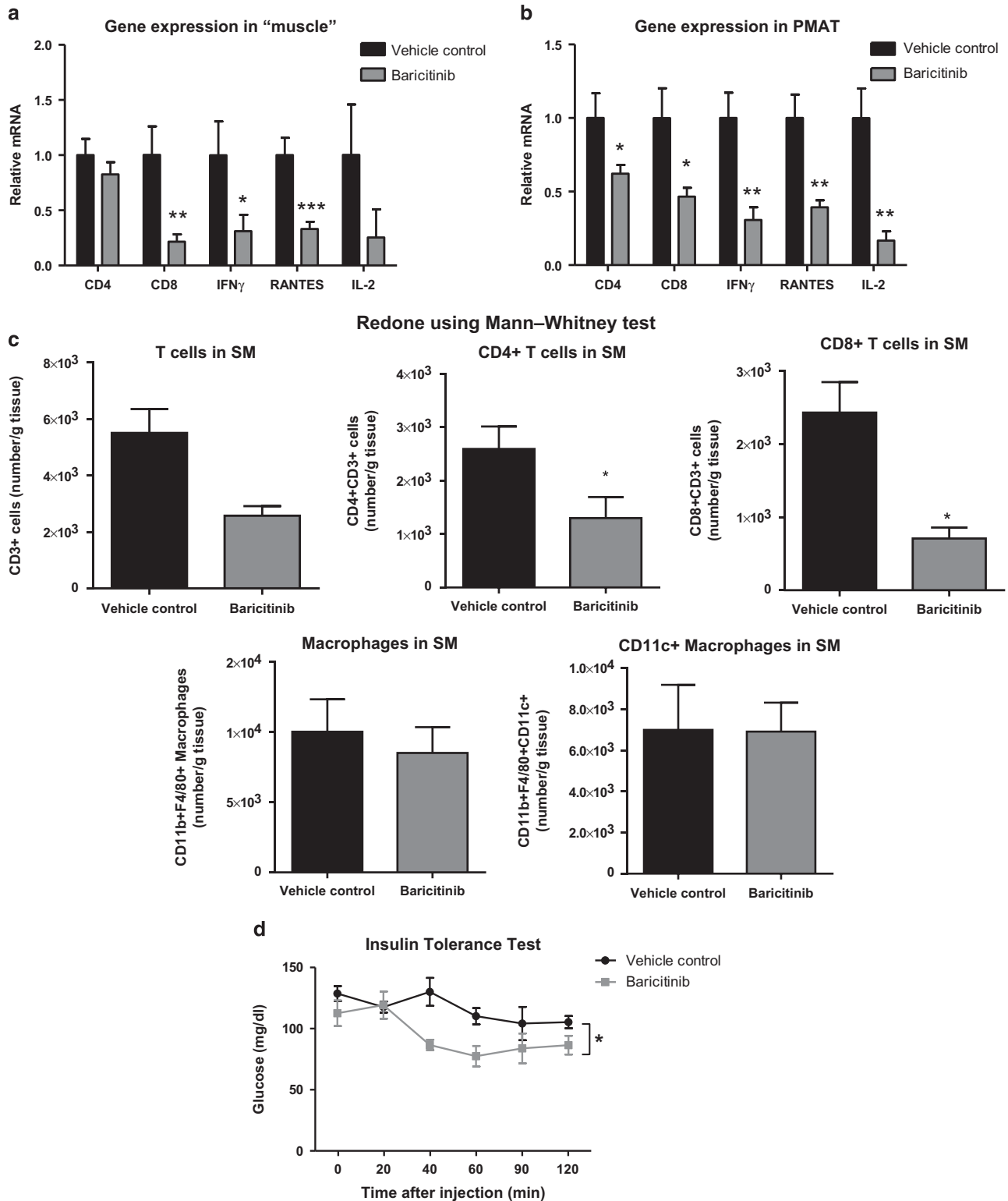


Figure 6. The effect of selective JAK1/JAK2 inhibition on SM inflammation and insulin sensitivity in HFD-fed mice. Obese WT mice were administered a selective JAK1 and JAK2 inhibitor, baricitinib, in a dose of 10 mg kg⁻¹ or vehicle control by oral gavage for 21 days. RNA was isolated from PMAT and 'muscle' of baricitinib- and vehicle control-treated HFD-fed mice ($n=8$ mice per group). RT-PCR analysis of T-cell markers in (a) 'muscle' and (b) PMAT. Flow cytometry was performed to quantify the numbers of total CD3+, CD4+ and CD8+ T cells and CD11b+F4/80+ and CD11b+F4/80+CD11c+ M1 macrophages per gram tissue ($n=5$ mice per group) in (c) SM of vehicle control- and baricitinib-treated mice. (d) Intraperitoneal insulin tolerance test (1.5 U kg⁻¹) ($n=5$ mice per group). * $P < 0.05$, ** $P < 0.01$, *** $P < 0.001$. Two-way ANOVA was performed to compare the response to insulin in vehicle control- and baricitinib-treated mice.

important role of T cells in obesity-induced SM inflammation. Future study needs to determine the 'signals' (such as chemokines) in SM that promote T-cell infiltration.

Our previous study revealed an important role of $\alpha\beta$ T cells in obesity-associated SM inflammation.³⁹ To study $\alpha\beta$ T cells in SM in more detail, we quantified both CD4+ and CD8+ T-cell subsets and revealed that obesity increased both CD4+ and CD8+ T-cell numbers. Similar to VAT,¹⁴ we found that within the CD4+ T-cell population, T_{reg} cells were markedly decreased, whereas T_H1 cells were increased in SM of obese mice. IFN γ and CD4 gene expression were upregulated in both 'muscle' and PMAT, but much greater increase in PMAT suggests that T_H1 cells were located primarily in muscle tissue adipose depots. We hypothesized that proinflammatory mediators released by T_H1 cells affect SM metabolic functions. Previous studies indicated that IFN γ contributes to adipocyte inflammation and insulin resistance through the JAK/STAT pathway.^{16,50} Our study demonstrated that T_H1 upregulated genes encoding inflammatory mediators, such as MCP-1, RANTES, IL-6 and TNF α , in myocytes and that this effect can be attributed to the presence of IFN γ . We observed that T_H1 -conditioned medium reduced insulin-stimulated Akt phosphorylation in C2C12 cells dependent on IFN γ . Inhibition of the JAK/STAT pathway attenuated T_H1 -induced inflammatory gene expression and restored insulin signaling in C2C12 myotubes. Consistent with these *in vitro* data and *in vivo* increases in T_H1 cells, we found higher levels of P-STAT1 in SM of obese mice, which was associated with increased inflammation and decreased insulin sensitivity. More importantly, to show the relevance of the IFN γ pathway *in vivo*, we used a selective JAK1/JAK2 inhibitor, baricitinib, currently in phase 3 clinical trials as a potential treatment for rheumatoid arthritis. Baricitinib administration resulted in marked reductions in SM T cells and IFN γ , the major T_H1 cytokine, consistent with an essential role of STAT1 in initiating T_H1 response.⁵¹ Despite marked T-cell marker reduction, baricitinib treatment did not impact macrophage markers, which was unexpected because of an essential role of STAT1 in M1 polarization.⁵² We speculate that short-term treatment may not be sufficient to alter macrophage polarization in SM of obese mice. Along with the reduced T cell-related inflammation, inhibition of the JAK/STAT pathway was also accompanied by improved insulin tolerance.

To our knowledge, we are the first to report the correlation of IMAT/PMAT in mouse leg muscle to homeostasis model assessment of insulin resistance, SM T-cell infiltration and insulin resistance. A limitation of this micro-CT experiment is a relatively small sample size. Nevertheless, we showed large differences in total IMAT/PMAT between lean and obese mice. Our study highlights that rapid expansion of EMAT is associated with insulin resistance and SM inflammation. EMAT is a predominant location of T cells, along with macrophages, that accumulate in SM of mice with diet-induced obesity. T cells and macrophages further impair metabolic functions of SM cells through a paracrine mechanism. Specifically, proinflammatory T_H1 cells may induce insulin resistance and increase inflammation in SM cells through a JAK/STAT mechanism.

In summary, the results of our study suggest that SM adipose depots (IMAT and PMAT) have altered phenotype, or 'adiposopathy', similar to that observed in VAT, and may have an important role in the development of insulin resistance, diabetes and inflammation associated with obesity.

CONFLICT OF INTEREST

The authors declare no conflict of interest.

ACKNOWLEDGEMENTS

This work was supported by NIH grants T32 GM88129 and T32 HL007812 (to IK), R01 HL098839 (to HW), P30 AI36211 (to DEL) and R01 DK078847 (to CMB). The authors thank Jerry L Perrard (Baylor College of Medicine) and Joshua Smith (Florida Hospital) for technical assistance, Ching H Tung, PhD (Houston Methodist Research Institute) for help with the CT imaging, Willa Hsueh, MD (Houston Methodist Research Institute) for donating mice for the micro-CT studies, Kerrie Jara (Baylor College of Medicine) for editorial assistance, Jacob Couturier (Department of Internal Medicine, UT Health, Houston, TX < USA) for help with the flow cytometry and the Mouse Metabolism Core at Baylor College of Medicine (under the Diabetes Research Center; supported by P30 DK079638) for help with insulin and glucose measurements. The authors also thank the human study participants.

REFERENCES

- Olefsky JM, Glass CK. Macrophages, inflammation, and insulin resistance. *Annu Rev Physiol* 2010; **72**: 219–246.
- Plomgaard P, Nielsen AR, Fischer CP, Mortensen OH, Broholm C, Penkowa M *et al*. Associations between insulin resistance and TNF-alpha in plasma, skeletal muscle and adipose tissue in humans with and without type 2 diabetes. *Diabetologia* 2007; **50**: 2562–2571.
- Lumeng CN, Bodzin JL, Saltiel AR. Obesity induces a phenotypic switch in adipose tissue macrophage polarization. *J Clin Invest* 2007; **117**: 175–184.
- Wu H, Perrard XD, Wang Q, Perrard JL, Polsani VR, Jones PH *et al*. CD11c expression in adipose tissue and blood and its role in diet-induced obesity. *Arterioscler Thromb Vasc Biol* 2009; **30**: 186–192.
- Xu H, Barnes GT, Yang Q, Tan G, Yang D, Chou CJ *et al*. Chronic inflammation in fat plays a crucial role in the development of obesity-related insulin resistance. *J Clin Invest* 2003; **112**: 1821–1830.
- Feinstein R, Kanety H, Papa MZ, Lunenfeld B, Karasik A. Tumor necrosis factor-alpha suppresses insulin-induced tyrosine phosphorylation of insulin receptor and its substrates. *J Biol Chem* 1993; **268**: 26055–26058.
- Wu H, Ghosh S, Perrard XD, Feng L, Garcia GE, Perrard JL *et al*. T-cell accumulation and regulated on activation, normal T cell expressed and secreted upregulation in adipose tissue in obesity. *Circulation* 2007; **115**: 1029–1038.
- Rausch ME, Weisberg S, Vardhana P, Tortorello DV. Obesity in C57BL/6J mice is characterized by adipose tissue hypoxia and cytotoxic T-cell infiltration. *Int J Obes (Lond)* 2008; **32**: 451–463.
- Kintscher U, Hartge M, Hess K, Foryst-Ludwig A, Clemenz M, Wabitsch M *et al*. T-lymphocyte infiltration in visceral adipose tissue: a primary event in adipose tissue inflammation and the development of obesity-mediated insulin resistance. *Arterioscler Thromb Vasc Biol* 2008; **28**: 1304–1310.
- Nishimura S, Manabe I, Nagasaki M, Eto K, Yamashita H, Ohsugi M *et al*. CD8+ effector T cells contribute to macrophage recruitment and adipose tissue inflammation in obesity. *Nat Med* 2009; **15**: 914–920.
- Deng T, Lyon CJ, Minze LJ, Lin J, Zou J, Liu JZ *et al*. Class II major histocompatibility complex plays an essential role in obesity-induced adipose inflammation. *Cell Metab* 2013; **17**: 411–422.
- Strissel KJ, DeFuria J, Shaul ME, Bennett G, Greenberg AS, Obin MS. T-cell recruitment and Th1 polarization in adipose tissue during diet-induced obesity in C57BL/6 mice. *Obesity (Silver Spring)* 2010; **18**: 1918–1925.
- Jiang E, Perrard XD, Yang D, Khan IM, Perrard JL, Smith CW *et al*. Essential role of CD11a in CD8+ T-cell accumulation and activation in adipose tissue. *Arterioscler Thromb Vasc Biol* 2014; **34**: 34–43.
- Feurerer M, Herrero L, Cipolletta D, Naaz A, Wong J, Nayer A *et al*. Lean, but not obese, fat is enriched for a unique population of regulatory T cells that affect metabolic parameters. *Nat Med* 2009; **15**: 930–939.
- Winer S, Chan Y, Paltser G, Truong D, Tsui H, Bahrami J *et al*. Normalization of obesity-associated insulin resistance through immunotherapy. *Nat Med* 2009; **15**: 921–929.
- McGillcuddy FC, Chiquoine EH, Hinkle CC, Kim RJ, Shah R, Roche HM *et al*. Interferon gamma attenuates insulin signaling, lipid storage, and differentiation in human adipocytes via activation of the JAK/STAT pathway. *J Biol Chem* 2009; **284**: 31936–31944.
- Xu H, Sethi JK, Hotamisligil GS. Transmembrane tumor necrosis factor (TNF)-alpha inhibits adipocyte differentiation by selectively activating TNF receptor 1. *J Biol Chem* 1999; **274**: 26287–26295.
- Souza SC, Palmer HJ, Kang YH, Yamamoto MT, Muliro KV, Paulson KE *et al*. TNF-alpha induction of lipolysis is mediated through activation of the extracellular signal related kinase pathway in 3T3-L1 adipocytes. *J Cell Biochem* 2003; **89**: 1077–1086.
- Guilherme A, Virbasius JV, Puri V, Czech MP. Adipocyte dysfunctions linking obesity to insulin resistance and type 2 diabetes. *Nat Rev Mol Cell Biol* 2008; **9**: 367–377.

- 20 Pillon NJ, Bilan PJ, Fink LN, Klip A. Cross-talk between skeletal muscle and immune cells: muscle-derived mediators and metabolic implications. *Am J Physiol Endocrinol Metab* 2013; **304**: E453–E465.
- 21 DeFronzo RA, Tripathy D. Skeletal muscle insulin resistance is the primary defect in type 2 diabetes. *Diabetes Care* 2009; **32**: S157–S163.
- 22 Ryder JW, Gilbert M, Zierath JR. Skeletal muscle and insulin sensitivity: pathophysiological alterations. *Front Biosci* 2001; **6**: D154–D163.
- 23 Pan DA, Lillioja S, Kriketos AD, Milner MR, Baur LA, Bogardus C *et al*. Skeletal muscle triglyceride levels are inversely related to insulin action. *Diabetes* 1997; **46**: 983–988.
- 24 Storlien LH, Jenkins AB, Chisholm DJ, Pascoe WS, Khouri S, Kraegen EW. Influence of dietary fat composition on development of insulin resistance in rats. Relationship to muscle triglyceride and omega-3 fatty acids in muscle phospholipid. *Diabetes* 1991; **40**: 280–289.
- 25 Goodpaster BH, Thaete FL, Simoneau JA, Kelley DE. Subcutaneous abdominal fat and thigh muscle composition predict insulin sensitivity independently of visceral fat. *Diabetes* 1997; **46**: 1579–1585.
- 26 Krssak M, Falk Petersen K, Dresner A, DiPietro L, Vogel SM, Rothman DL *et al*. Intramyocellular lipid concentrations are correlated with insulin sensitivity in humans: a ¹H NMR spectroscopy study. *Diabetologia* 1999; **42**: 113–116.
- 27 Perseghin G, Scifo P, De Cobelli F, Pagliato E, Battezzati A, Arcelloni C *et al*. Intramyocellular triglyceride content is a determinant of *in vivo* insulin resistance in humans: a ¹H-¹³C nuclear magnetic resonance spectroscopy assessment in offspring of type 2 diabetic parents. *Diabetes* 1999; **48**: 1600–1606.
- 28 Moro C, Bajpeyi S, Smith SR. Determinants of intramyocellular triglyceride turnover: implications for insulin sensitivity. *Am J Physiol Endocrinol Metab* 2008; **294**: E203–E213.
- 29 Sinha R, Dufour S, Petersen KF, LeBon V, Enoksson S, Ma YZ *et al*. Assessment of skeletal muscle triglyceride content by (1)H nuclear magnetic resonance spectroscopy in lean and obese adolescents: relationships to insulin sensitivity, total body fat, and central adiposity. *Diabetes* 2002; **51**: 1022–1027.
- 30 Goodpaster BH, Thaete FL, Kelley DE. Thigh adipose tissue distribution is associated with insulin resistance in obesity and in type 2 diabetes mellitus. *Am J Clin Nutr* 2000; **71**: 885–892.
- 31 Goss AM, Gower BA. Insulin sensitivity is associated with thigh adipose tissue distribution in healthy postmenopausal women. *Metabolism* 2012; **61**: 1817–1823.
- 32 Varma V, Yao-Borengasser A, Rasouli N, Nolen GT, Phanavanh B, Starks T *et al*. Muscle inflammatory response and insulin resistance: synergistic interaction between macrophages and fatty acids leads to impaired insulin action. *Am J Physiol Endocrinol Metab* 2009; **296**: E1300–E1310.
- 33 Hevener AL, Olefsky JM, Reichart D, Nguyen MT, Bandyopadhyay G, Leung HY *et al*. Macrophage PPAR gamma is required for normal skeletal muscle and hepatic insulin sensitivity and full antidiabetic effects of thiazolidinediones. *J Clin Invest* 2007; **117**: 1658–1669.
- 34 Patsouris D, Li PP, Thapar D, Chapman J, Olefsky JM, Neels JG. Ablation of CD11c-positive cells normalizes insulin sensitivity in obese insulin resistant animals. *Cell Metab* 2008; **8**: 301–309.
- 35 Fink LN, Costford SR, Lee YS, Jensen TE, Bilan PJ, Oberbach A *et al*. Pro-inflammatory macrophages increase in skeletal muscle of high fat-fed mice and correlate with metabolic risk markers in humans. *Obesity (Silver Spring)* 2013; **22**: 747–757.
- 36 Hong EG, Ko HJ, Cho YR, Kim HJ, Ma Z, Yu TY *et al*. Interleukin-10 prevents diet-induced insulin resistance by attenuating macrophage and cytokine response in skeletal muscle. *Diabetes* 2009; **58**: 2525–2535.
- 37 Bruun JM, Helge JW, Richelsen B, Stallknecht B. Diet and exercise reduce low-grade inflammation and macrophage infiltration in adipose tissue but not in skeletal muscle in severely obese subjects. *Am J Physiol Endocrinol Metab* 2006; **290**: E961–E967.
- 38 Tam CS, Sparks LM, Johannsen DL, Covington JD, Church TS, Ravussin E. Low macrophage accumulation in skeletal muscle of obese type 2 diabetics and elderly subjects. *Obesity (Silver Spring)* 2012; **20**: 1530–1533.
- 39 Khan IM, Dai Perrard XY, Perrard JL, Mansoori A, Wayne Smith C, Wu H *et al*. Attenuated adipose tissue and skeletal muscle inflammation in obese mice with combined CD4+ and CD8+ T cell deficiency. *Atherosclerosis* 2014; **233**: 419–428.
- 40 Wu H, Rodgers JR, Perrard XY, Perrard JL, Prince JE, Abe Y *et al*. Deficiency of CD11b or CD11d results in reduced staphylococcal enterotoxin-induced T cell response and T cell phenotypic changes. *J Immunol* 2004; **173**: 297–306.
- 41 Zhang Y, Pilon G, Marette A, Baracos VE. Cytokines and endotoxin induce cytokine receptors in skeletal muscle. *Am J Physiol Endocrinol Metab* 2000; **279**: E196–E205.
- 42 Stark GR, Kerr IM, Williams BR, Silverman RH, Schreiber RD. How cells respond to interferons. *Annu Rev Biochem* 1998; **67**: 227–264.
- 43 Luu YK, Lublinsky S, Ozcivici E, Capilla E, Pessin JE, Rubin CT *et al*. *In vivo* quantification of subcutaneous and visceral adiposity by micro-computed tomography in a small animal model. *Med Eng Phys* 2009; **31**: 34–41.
- 44 Fink LN, Oberbach A, Costford SR, Chan KL, Sams A, Blucher M *et al*. Expression of anti-inflammatory macrophage genes within skeletal muscle correlates with insulin sensitivity in human obesity and type 2 diabetes. *Diabetologia* 2013; **56**: 1623–1628.
- 45 Fridman JS, Scherle PA, Collins R, Burn TC, Li Y, Li J *et al*. Selective inhibition of JAK1 and JAK2 is efficacious in rodent models of arthritis: preclinical characterization of INCB028050. *J Immunol* 2010; **184**: 5298–5307.
- 46 Strissel KJ, Stancheva Z, Miyoshi H, Perfield JW 2nd, DeFuria J, Jick Z *et al*. Adipocyte death, adipose tissue remodeling, and obesity complications. *Diabetes* 2007; **56**: 2910–2918.
- 47 Gunn MD, Nelken NA, Liao X, Williams LT. Monocyte chemoattractant protein-1 is sufficient for the chemotaxis of monocytes and lymphocytes in transgenic mice but requires an additional stimulus for inflammatory activation. *J Immunol* 1997; **158**: 376–383.
- 48 Schall TJ, Bacon K, Toy KJ, Goeddel DV. Selective attraction of monocytes and T lymphocytes of the memory phenotype by cytokine RANTES. *Nature* 1990; **347**: 669–671.
- 49 Ley K, Laudanna C, Cybulsky MI, Nourshargh S. Getting to the site of inflammation: the leukocyte adhesion cascade updated. *Nat Rev Immunol* 2007; **7**: 678–689.
- 50 Rocha VZ, Folco EJ, Sukhova G, Shimizu K, Gotsman I, Vernon AH *et al*. Interferon-gamma, a Th1 cytokine, regulates fat inflammation: a role for adaptive immunity in obesity. *Circ Res* 2008; **103**: 467–476.
- 51 Schulz EG, Mariani L, Radbruch A, Hofer T. Sequential polarization and imprinting of type 1 T helper lymphocytes by interferon-gamma and interleukin-12. *Immunity* 2009; **30**: 673–683.
- 52 Sica A, Mantovani A. Macrophage plasticity and polarization: *in vivo* veritas. *J Clin Invest* 2012; **122**: 787–795.

Supplementary Information accompanies this paper on International Journal of Obesity website (<http://www.nature.com/ijo>)